AD-751 568

REVIEW OF THE MAGNETOSPHERIC WAVE-PARTICLE INTERACTION WORKSHOP, HELD AT STANFORD RESEARCH INSTITUTE, MENLO PARK, CALIFORNIA ON 11-13 JULY 1972

John F. Vesecky

Stanford Research Institute

Prepared for:

Defense Advanced Research Projects Agency

October 1972

Special Report

REVIEW OF THE MAGNETOSPHERIC WAVE-PARTICLE INTERACTION WORKSHOP

Held at STANFORD RESEARCH INSTITUTE
Menlo Park, California
11-13 July 1972

Prepared for:

OFFICE OF NAVAL RESEARCH
UNITED STATES NAVY
800 NORTH QUINCY STREET
ARLINGTON, VIRGINIA 22217

CONTRACT N00014-72-C-0402

Sponsored by

DEFENSE ADVANCED RESEARCH PROJECTS AGENCY
ARPA ORDER NO. 2141
11 FEBRUARY 1972

STANFORD RESEARCH INSTITUTE
Menlo Park, California 94025 · U.S.A.

60

R

Security Classification

DOCUMENT CONTROL DATA - R & D

(Security classification of title, body of abstract and indexing annotation must be entered when the overall report is classified)

1. ORIGINATING ACTIVITY (Corporate author)
Stanford Research Institute
Menlo Park, Calif.

2a. REPORT SECURITY CLASSIFICATION
Unclassified

2b. GROUP

3. REPORT TITLE
REVIEW OF THE MAGNETOSPHERIC WAVE-PARTICLE INTERACTION WORKSHOP
Held at Stanford Research Institute, Menlo Park, California, 11-13 July 1972

4. DESCRIPTIVE NOTES (Type of report and inclusive dates)
Special Report

5. AUTHOR(S) (First name, middle initial, last name)
John F. Vesecky

6. REPORT DATE
October 1972

7a. TOTAL NO OF PAGES
72

7b. NO OF REFS
14

8a. CONTRACT OR GRANT NO
Contract N00017-72-C-0402

b. PROJECT NO.

c.

d.

9a. ORIGINATOR'S REPORT NUMBER(S)
Special Report
SRI Project 1840

9b. OTHER REPORT NO(S) (Any other numbers that may be assigned this report)

10. DISTRIBUTION STATEMENT

11. SUPPLEMENTARY NOTES
Monitored by:
Office of Naval Research
Arlington, Virginia

12. SPONSORING MILITARY ACTIVITY
Defense Advanced Research Projects Agency
Arlington, Virginia

13. ABSTRACT

A workshop on magnetospheric wave-particle interaction sponsored by ARPA and ONR was held at Stanford Research Institute, Menlo Park, California on 11-13 July, 1972. The general view of the workshop participants was that significant wave amplification at ULF and VLF frequencies can be artificially stimulated by injecting cold plasma outside the plasmapause in the magnetosphere, and that specific military applications for such wave amplification (communications) and its associated particle precipitation (nuclear weapons effects) are possible. The following subjects were discussed: (1) potential military applications, (2) physics of the wave-amplifying mechanism, (3) experimental observations and current theory of ULF and VLF wave-particle interaction, and (4) design of experiments to investigate wave-particle interaction phenomena. It was also the view of the workshop participants that further research should be carried out to design an optimum experimental investigation of cold-plasma-injection phenomena. A detailed list of the necessary research topics was prepared and is included in this report.

Ia

DD FORM 1 NOV 68 1473 (PAGE 1)

S/N 0101-807-6801

Security Classification

14 KEY WORDS	LINK A		LINK B		LINK C	
	ROLE	WT	ROLE	WT	ROLE	WT
Magnetospheric physics						
VLF						
ULF						
Plasma instabilities						
Wave propagation						
Particle precipitation						

Ib

STANFORD RESEARCH INSTITUTE
Menlo Park, California 94025 · U.S.A.

Special Report

October 1972

REVIEW OF THE MAGNETOSPHERIC WAVE-PARTICLE INTERACTION WORKSHOP

Held at STANFORD RESEARCH INSTITUTE
Menlo Park, California
11-13 July 1972

Compiled by: JOHN F. VESECKY

Prepared for:

OFFICE OF NAVAL RESEARCH
UNITED STATES NAVY
800 NORTH QUINCY STREET
ARLINGTON, VIRGINIA 22217
Attention: DIRECTOR, PHYSICS BRANCH

Contract No. N00014-72-C-0402
ARPA Order No. 2141
Program Code No. 2F10
Principal Investigator: A. M. Peterson
(415) 326-6200 Ext. 3053
Contract Date: 1 March 1972 to 28 February 1973
Contract Amount: $74,486.00

SRI Project 1840

This research was supported by the Defense Advanced Research Projects Agency and was monitored by the Office of Naval Research under Contract No. N00014-72-C-0402.

Approved by:

DAVID A. JOHNSON, *Director*
Radio Physics Laboratory

RAY L. LEADABRAND, *Executive Director*
Electronics and Radio Sciences Division

Copy No. 13

III

LIST OF ATTENDEES

The people listed below attended the ARPA and ONR sponsored workshop on wave-particle interaction in the magnetosphere held at Stanford Research Institute, July 11-13, 1972 and contributed material to this report.

Mr. Loren S. Bearce	Naval Research Laboratory
Dr. William E. Blair	Stanford Research Institute
Dr. Neil Brice	Cornell University
Mr. George B. Carpenter	Stanford Research Institute
Dr. John M. Cornwall	Aerospace Corporation and UCLA
Dr. John G. Dardis	Office of Naval Research
Dr. Edward C. Field, Jr.	Pacific-Sierra Research Corporation
Dr. Anthony C. Fraser-Smith	Stanford University
Dr. Harold B. Liemohn	Battelle Pacific Northwest Laboratories
Dr. Billy M. McCormac	Lockheed Palo Alto Research Laboratory
Dr. Allen M. Peterson	Stanford Research Institute
Dr. Walter H. Podney	Physical Dynamics, Inc.
Dr. H. Michael Schulz	Aerospace Corporation
Dr. John F. Vesecky	Stanford Research Institute
Dr. Martin Walt	Lockheed Palo Alto Research Laboratory
Dr. Thomas N. C. Wang	Stanford Research Institute

CONTENTS

ILLUSTRATIONS

TABLES

ACKNOWLEDGMENTS

The editor would like to thank all the workshop participants both for providing material to be used in the report and for making many valuable comments and suggestions in response to the preliminary draft. Dr. J. G. Dardis of ONR was particularly helpful as Chairman during the workshop meetings and in completing the final document. The editor also gratefully acknowledges the able assistance of Mrs. F. P. Beauchamp and Dr. W. E. Blair in the preparation and final editing of the report.

ACRONYMS, SYMBOLS, AND ABBREVIATIONS

A	Particle anisotropy
Å	Angstrom unit, 10^{-10} meters
ABM	Anti Ballistic Missile
AEC	Atomic Energy Commission
ARPA	Defense Advanced Research Projects Agency
B	Magnetic field strength
c	Speed of light
dB	Decibel
cm	Centimeter
DoD	Department of Defense
E	Particle energy
ELF	Extremely low frequency, 30 Hz to 3 kHz
ESRO	European Satellite Resea ch Organization
e	Charge on an electron
el	Electron
eV	Electron volt (1.602×10^{19} joules)
HF	High frequency, 3 to 30 MHz
H_α	First Balmer emission from hydrogen
Hz	Hertz, one cycle per second
K	Temperature in Kelvin
K_p	Magnetic index
k	Wave number
keV	Kiloelectronvolt
kHz	Kilohertz, 1000 hertz
km	Kilometer, 1000 meters
km/s	Kilometer/second, 1000 meters per second

Li	Lithium
LF	Low frequency, 30 to 300 kilohertz
Loss cone	A cone whose axis coincides with the local geomagnetic-field direction. Particles having velocity vectors inside the loss cone will precipitate into the lower atmosphere as they approach the earth rather than mirroring, as shown in Figure 2.
L Shell	A surface generated by rotating a geomagnetic field line about the earth's dipole axis. The equatorial radial distance, measured in earth radii, of this shell from the dipole axis is designated L.
MeV	Megaelectronvolt
MHz	Megahertz
m	Meter
N	Particle density
n	Refractive index = c/V_p = speed of light/wave phase velocity.
NASA	National Aeronautics and Space Administration
NSF	National Science Foundation
OHD	Over-the-Horizon-Detection
ONR	Office of Naval Research
R_E	Distance in multiples of earth's radius
SE	Seattle, Washington
SRI	Stanford Research Institute
s	Second
sr	Steradian
sub LF	Frequencies below 30 kHz
UT	Universal time
UV	Ultraviolet
UHF	Ultra high frequency, 300 MHz to about 800 MHz
ULF	Ultra low frequency, usually defined as below 30 Hz, taken to mean 0.1 to 5 Hz for the purposes of this report.
V_g	Group velocity
V_p	Phase velocity

VLF	Very low frequency, usually defined as 3 to 30 kHz, taken to mean 100 Hz to 10 kHz for the purposes of this report.
VHF	Very high frequency, 30 to 300 MHz
W	Wave energy
W/m^2	Watt per square meter
Π	Plasma frequency
ϵ_o	Permittivity of free space
ω	Wave frequency
γ	Growth rate
ℓ	Length of amplifying region
μ_o	Permeability of free space
Ω	Cyclotron frequency

I SUMMARY AND RECOMMENDATIONS

A workshop on magnetospheric wave-particle interaction under joint sponsorship of ARPA and ONR met 11-13 July 1972 at Stanford Research Institute, Menlo Park, California. The people who attended the meeting and contributed to this report are listed in List of Attendees. The following areas were considered: (1) defense applications of magnetospheric ULF and VLF wave amplification and of particle precipitation, (2) physics of the amplifying mechanism, (3) experimental observation and current theory of ULF and VLF wave-particle interaction, and (4) design of experiments to investigate wave-particle interaction phenomena. The report of the workshop is correspondingly divided into four sections, each of which is summarized below. Recommendations follow this summary.

A. Summary

1. Defense Applications of Magnetospheric Wave Amplification and Particle Precipitation

At present, frequencies below about 100 Hz probably provide the most realistic hope of communicating with deeply submerged submarines. Due to the exceedingly long wavelength it is very difficult to radiate sub-LF ($\lesssim$30 kHz) waves efficiently from ground-based or satellite transmitters. It is thus evident that a high payoff would be realized if the ability of the magnetosphere to act as a ULF/VLF amplifier could be utilized. It is important that this be assessed.

High-altitude nuclear explosions inject radioactive particles into the magnetosphere where they can be trapped for months to years. The artificially stimulated precipitation (dumping into the lower atmosphere) of these particles would enhance the survivability of

satellites that must survive in the magnetosphere. Artificial precipitation by the injection of cold plasma therefore seems to be a technique well worth pursuing. These two areas--amplification of sub-LF waves and precipitation of trapped particles appear at present to hold promise as defense application for magnetospheric wave-particle interactions stimulated by cold plasma injection.

2. Physics of the Amplifying Mechanism

Energy from the solar wind is injected into the Earth's magnetosphere and stored as energetic trapped particles in the trapped-particle (Van Allen) belts, some 10^{15} Joules being stored. A small fraction of this energy is converted into natural electromagnetic waves in the 0.1-to-1-Hz (ULF) and 100-Hz-to-10-kHz (VLF)* frequency ranges. On occasion these waves are greatly amplified by naturally occurring plasma instabilities. This wave-growth process is accompanied by particle precipitation--that is, energetic particles escape the trapped particle belts and deposit their energy on collision with atoms in the lower atmosphere (~100 km altitude). This naturally occurring process is thought to be the result of a wave-particle interaction known as cyclotron resonance. In this process ULF waves interact with energetic protons and VLF waves interact with energetic electrons spiraling around geomagnetic field lines, but traveling in a direction opposite to the waves. At resonance the particle perceives the wave-frequency Doppler shifted up to its own cyclotron frequency (the frequency with which it circles the magnetic field line) and some of the particle energy is (on average) transferred to the wave, thus amplifying it. In addition, the particle velocity typically becomes directed more nearly along the magnetic field line, making the average particle more likely to precipitate. For a given wave frequency the amount of amplification and precipitation

*Though VLF is usually defined as 3 to 30 kHz we shall extend this definition to cover the 100-Hz-to-10-kHz range for the purposes of this report.

transferred to the wave, thus amplifying it. In addition, the particle velocity typically becomes directed more nearly along the magnetic field line, making the average particle more likely to precipitate. For a given wave frequency the amount of amplification and precipitation is proportional to the number of energetic particles that can resonate with that wave frequency. The number of energetic particles available for resonance can be increased by slowing down the wave, more trapped particles are available at the lower energies to resonate with the slower waves. Since we can artificially amplify ULF and VLF waves in the magnetosphere, we cause artificial particle precipitation as shown in Section IV-B (Figure 4).

3. Experimental Observations and Current Theory of ULF and VLF Wave-Particle Interaction

Cyclotron resonance between waves and particles in the natural magnetosphere has received much experimental and theoretical attention in the past few years. Experimental investigations have shown that at times strongly amplified ULF and VLF waves occur naturally in the magnetosphere and that particle precipitation is associated with natural increases in the magnetospheric cold-plasma density. An example of natural magnetospheric VLF wave amplification via cyclotron resonance is the long-enduring whistler echo train shown in Section V-A (Figure 5). Here the VLF waves bounce back and forth along the geomagnetic field lines many times (about 210 times in Figure 5), with the reflection loss in the lower ionosphere partially counteracted by wave amplification in the outer magnetospheric portion of the propagation path. A corresponding ULF event is the hydromagnetic whistler (or pearl micropulsation) discussed in Section V-A (see Figure 6). Here, ULF waves bouncing back and forth along field lines are observed to grow in amplitude due to amplification involving cyclotron resonance.

The physics of ULF and VLF amplification by cyclotron-resonant interactions is now well enough understood that reliable estimates can be made quickly of many of the relevant parameters needed for the evaluation of proposed experiments. Computer programs to make detailed wave-growth calculations now exist. For example, by making a few suitable approximations it can be shown that for the case of artificial ULF amplification by lithium-vapor injection near the equatorial plane at a geocentric distance of 6.6 earth radii, the number density of lithium ions needed for significantly enhanced amplification is given by $N_{Li} \approx 46/\bar{E}_p$ cm^{-3}, where $\bar{E}_p$ is the mean proton energy in keV. Typically, $\bar{E}_p \approx 20$ keV and $N_{Li} \approx 2$ to 3 cm^{-3}.

As an example of more detailed wave-growth calculations, consider a technically feasible lithium injection at 6.6 earth radii near the equatorial plane. For an injected lithium ion density of 3 cm^{-3} over a 7000-km-long column along geomagnetic field lines, wave-amplification calculations using data from satellite measurements of magnetospheric protons show a ULF gain of between 30 and 40 dB at a frequency of about 0.2 Hz.

4. Design of Experiments to Investigate Wave-Particle Interaction Phenomena

It appears to be possible to carry out experiments in space to investigate the amount of ULF/VLF wave amplification and particle precipitation caused by artificial cold-plasma injection. The experimental concepts are sound and there appears to be no fundamental uncertainty or obstacle.

Successful experiments using cold-plasma injection to stimulate ULF and VLF wave amplification should be such that the amplification volume is near the equatorial plane and the cold plasma background is

low enough that the plasma injected constitutes a major perturbation. Further, the ambient energetic particle flux in the amplifying region must not be too low or too disturbed. Drift separation between the injected ion cloud and the spacecraft is undesirable.

The measurements required to determine the amount of ULF or VLF amplification and particle precipitation following plasma injection are listed in Table 1.

Table 1

REQUIRED MEASUREMENTS

For ULF Amplification Experiment	For VLF Amplification Experiment	Platform
Proton environment in amplifying volume	Electron environment in amplifying volume	Spacecraft
Li injection	Cold-plasma injection	Spacecraft
Li ion distribution	Ion distribution	Spacecraft/ground
Li neutral distribution	Neutral distribution	Ground
ULF waves	VLF waves	Spacecraft/ground
Proton precipitation	Electron precipitation	Ground/balloon

Such measurements would provide for a meaningful comparison between theory and observation so that design parameters for future system applications could be defined.

Ground-based wave-transmission experiments could also be used to study wave-particle interaction in the magnetosphere. Such experiments could determine the optimum frequency and waveform for stimulating VLF emissions and electron precipitation, how frequently this

process occurs, and whether the emission of waves significantly alters the properties of the energetic particles (that is, whether one emission substantially reduces the wave growth rate, inhibiting subsequent emissions, and if so, what is the "recovery time?").

B. Conclusions and Recommendations

It was the view of the workshop participants that significant wave amplification at ULF and VLF frequencies can be achieved by plasma injection outside the plasmapause, and that specific military applications for wave amplification (communications) and particle precipitation (nuclear weapons effects) are possible. The workshop concluded, further, that the naturally occurring wave-amplifying region outside the plasmapause can be used for investigating magnetospheric-ionospheric coupling, which has general applications to military operations in the space environment. It was also concluded that more research should be carried out to calculate the needed parameters and to work out the experimental design for an optimum experimental investigation of this effect. Such a calculational and experimental design program in magnetospheric physics would not be expensive (not more than about $500,000 per year), and would complement and enhance DoD relevance of certain existing and proposed experimental programs of NSF, AEC, Navy and NASA.

A well designed experimental program would provide needed observational feedback so that present theory can be confirmed and extended or modified in the light of experimental evidence. Detailed topics recommended for further study are as follows.

(1) Calculations of ULF and VLF Wave Generation, Amplification, and Propagation

- Make the ULF and VLF wave-amplification calculations necessary to design an optimum wave-particle interaction

experiment and to interpret the experimental observations in order to determine the magnitude of wave growth and particle precipitation. Examine the following specific problems: (a) the effect on wave growth rate of secondary instabilities, nonlinear processes, and gradients and striations in the injected plasma cloud, and (b) conditions under which plasma injection will generate ULF or VLF waves.

- Examine the wave-propagation properties of ULF and VLF waves necessary to design an optimum plasma-injection experiment, including (a) reflection and transmission properties of the ionosphere for ULF and VLF waves, and (b) oblique wave propagation such as cyclotron and Landau wave-particle interaction, so that the effects of losses from and multiple passes through the amplifying region can be determined.

(2) Investigation of Experimental Design Parameters

- Investigate ion-cloud release dynamics (size and shape of cloud, existence of striations, time to reach equilibrium in a realistic model magnetosphere, and electric convection fields) to determine optimum design criteria for future experiments.

- Determine design criteria for lithium release by shaped charges from rockets and thermite canisters from satellites, to evaluate the relative merits of each.

- Examine techniques of measuring the location and structure of the injected plasma cloud; in particular, calculate the X-ray fluorescence of lithium ions and compare the resonance-scattering emission of lithium, barium, and barium ions with available instrumentation.

- Investigate techniques of measuring the predicted electron and proton precipitations, such as phase sounder, photometry, and backscatter radar.
- Examine the relative merits of satellite and ground-based measurements of ULF and VLF waves.
- Examine the usefulness of ground-based ULF and VLF wave transmission experiments.

(3) Analysis of Existing Data on Magnetospheric Particles and Waves

- Analyze existing magnetospheric electron and proton data (both hot and cold plasma) to select experimental release conditions such that the probability of having an acceptable ambient environment at plasma injection is high.
- Examine existing data on magnetospheric electric fields, so that the magnitude of convective motion of the released plasma cloud can be determined.
- Examine existing data on natural ULF and VLF noise amplitudes to optimize release conditions so that the ULF and VLF inputs to the wave-particle amplifying region will be sufficiently large to cause an easily observed output.

(4) Analysis of Related Experimental Programs

- Examine related experimental programs funded by other agencies (e.g., AEC, NSF, Navy, ESRO, and NASA) to obtain relevant new experimental information and to be aware of opportunities for possible experimental participation.

- Examine instrumentation, both ground-based and carried by existing and proposed satellites, such as ATS-5 and ATS-6, in order to note sensors that are potentially useful in future wave-particle interaction experiments.

- Give adequate support to ground-based VLF wave transmission facilities now being constructed at Siple, Antarctic with receiving facilities at Roberval, Canada under NSF sponsorship, and at Port Heiden, Alaska with receiving facilities at Dunedin, New Zealand under Navy sponsorship. This should be done so that the program can function effectively in providing data relevant to VLF amplification experiment design.

II INTRODUCTION

A workshop under joint ARPA and ONR sponsorship met on the 11th, 12th, and 13th of July 1972 at Stanford Research Institute to discuss artificially stimulated wave amplification and particle precipitation in the magnetosphere. This report gives the consensus views of the workshop participants, who are listed in the List of Attendees.

In the natural magnetosphere, wave-particle interactions and cyclotron resonance in particular have been studied extensively both experimentally and theoretically in the past few years. These investigations show that strongly amplified ULF and VLF waves occur naturally in the magnetosphere and are often accompanied by increases in the precipitation of trapped particles into the lower atmosphere. As understanding of these natural processes in the magnetosphere has increased, it has become evident that significant ULF and VLF wave amplification and associated particle precipitation can be stimulated artificially by the injection of relatively small amounts of cold plasma into the portion of the trapped-particle belts just outside the plasmapause in the magnetosphere. Possible military applications for wave amplification (ULF and VLF communication) and particle precipitation (dumping of particles injected by high-altitude nuclear explosions) are discussed. The group agreed that further research should be carried out to calculate the necessary parameters and work out the design for an optimum experimental investigation of the aforementioned effects.

III DEFENSE APPLICATIONS OF MAGNETOSPHERIC ULF AND VLF WAVE AMPLIFICATION AND PARTICLE PRECIPITATION

Energy from the solar wind in the form of energetic particles is injected into the earth's magnetosphere at a rate of about 10^{11} joules per second, with the stored energy in the magnetosphere (being typically about 10^{15} joules). Most of the energy lost from the magnetosphere is deposited in the upper atmosphere when energetic particles, lost from the trapped-radiation belts, collide with neutral atoms or molecules. A small fraction of the magnetospheric energy is converted into electromagnetic waves primarily in two frequency ranges, 0.1 to 5 Hz (ULF emissions) and 100 Hz to 10 kHz (VLF emissions). On occasion, these waves are greatly amplified by naturally occurring plasma instabilities. This wave growth process is often accompanied by increased precipitation of particles from the trapped particle belts into the lower atmosphere--electrons in the case of VLF waves and protons in the case of ULF waves. The purpose of plasma and wave-injection experiments is to determine to what extent these naturally occurring plasma instabilities that produce wave amplification and particle precipitation can be controlled for useful defense applications.

The military applications that appear at this time to hold the most promise are amplification of ULF/VLF communication signals and protection of satellites by controlled precipitation (dumping) of energetic trapped electrons injected by high-altitude nuclear explosions. These applications are discussed briefly below, and some others of more marginal promise are mentioned.

A. Enhancement of ULF/VLF Communications via Cold-Plasma Injection

It is widely recognized that frequencies below 100 Hz probably provide the most realistic hope of communicating with deeply submerged submarines, since waves of higher frequency are heavily attenuated in sea water. Further, one is driven to ELF or ULF in order to penetrate into the sea through the lower ionosphere in certain nuclear environments. Due to the immense wavelength, it is very difficult to radiate ULF waves efficiently from either ground-based or satellite transmitters. No practical transmitter of ULF waves exists today. The potential utility of a ULF communication system, and the difficulty of obtaining adequate radiated power by conventional means, clearly indicate the high payoff that would be realized if the ability of the magnetosphere to act as a ULF amplifier could be utilized and/or controlled. It is important that this be assessed.

Even at VLF it is unknown whether adequate power can be radiated from a satellite. This problem has been receiving attention in the defense community in conjunction with a possible future sub-LF satellite system that would be used to communicate to submarines. The possibly severe power requirements would be substantially alleviated if (1) waves were amplified in the magnetosphere subsequent to being radiated, and (2) significant guidance of these waves by geomagnetic-field-aligned ducts of ionization could be relied upon. A cold ($\sim$1500°K) plasma injection experiment, with related theoretical and experimental work, could determine the feasibility of controlling or enhancing wave amplification and guidance. If control is possible, the chances of developing a practical VLF/ULF satellite communication system would be significantly improved.

B. Precipitation of Energetic Electrons from a Nuclear Explosion

High-altitude nuclear detonations introduce intense shells of trapped electrons whose distributions and decay rates are influenced by wave-particle interactions. A better knowledge of these interactions is needed to improve estimates of the wartime trapped-electron environment. In particular, present estimates of the maximum possible flux of trapped electrons are uncertain by at least an order of magnitude due to lack of confidence in the calculation of precipitation rates. Survivable satellites must operate while being irradiated. Particle precipitation stimulated by cold-plasma injection might significantly reduce the radiation dose to which such satellites would be exposed. An increased knowledge of both natural and artificially stimulated wave-particle interactions should therefore lower the specifications to which satellites must be designed, with a consequent saving of equipment costs or an increase in reliability.

Formation of an artificial plasma cloud has some tactical application that could prove useful. For example, a synchronous satellite might be protected from trapped electrons if a plasma cloud were released on the same L shell but to the west of the satellite and east of the detonation point. Even if complete particle precipitation (dumping) during one longitudinal drift period were not possible, it is very likely that the time-integrated dose to the satellite could be reduced. Another tactical application might be to inject the plasma at low altitude west of the region where ABM intercepts are to occur. Although an ABM would not be damaged by precipitating electrons, performance of some guidance sensors can be seriously degraded by an intense electron flux.

In addition to the two items just discussed, it is possible that enhanced ionospheric ionization caused by precipitated electrons would cause (1) either enhancement or degradation on long-range, HF communication links, (2) disruption of OHD radar performance, (3) increased

absorption of transionospheric sub-LF communication signals, and (4) increased scintillation of transionospheric VHF and UHF communications signals.

IV PHYSICS OF THE AMPLIFYING MECHANISM

This section gives a brief review of the physics underlying the cyclotron-resonance interaction responsible for wave amplification and particle precipitation in the magnetosphere. Background information concerning the trapped-particle belts, the natural frequencies of plasma particles, and ULF/VLF wave propagation is followed by an explanation of cyclotron-resonance instability and how it can be stimulated by the injection of cold plasma.

A. Background

Figure 1 illustrates the earth's magnetosphere extending from about 1,500 km to 10 earth radii and containing nearly fully ionized plasma. Energetic, hot (keV to MeV) electrons and ions are trapped by the earth's magnetic field in radiation belts (the Van Allen belts). A cold (eV) thermal background plasma is also present. This cold plasma is contained mainly within the plasmapause, outside of which the cold-plasma density drops by more than an order of magnitude--from $\sim$500 cm^{-3} inside to $\sim$1 cm^{-3} outside.

The motion of particles trapped on a magnetic field line can be separated into three components (see Figure 2): (1) gyration around the field line at the angular cyclotron frequency

$$\Omega = eB/m \qquad (1)$$

where e and m are the particle charge and mass, respectively, and B is the magnetic flux density (MKS units are used throughout this report, unless specified otherwise); (2) bouncing back and forth along the field line between the mirror points (M_1 and M_2) at which the particle is

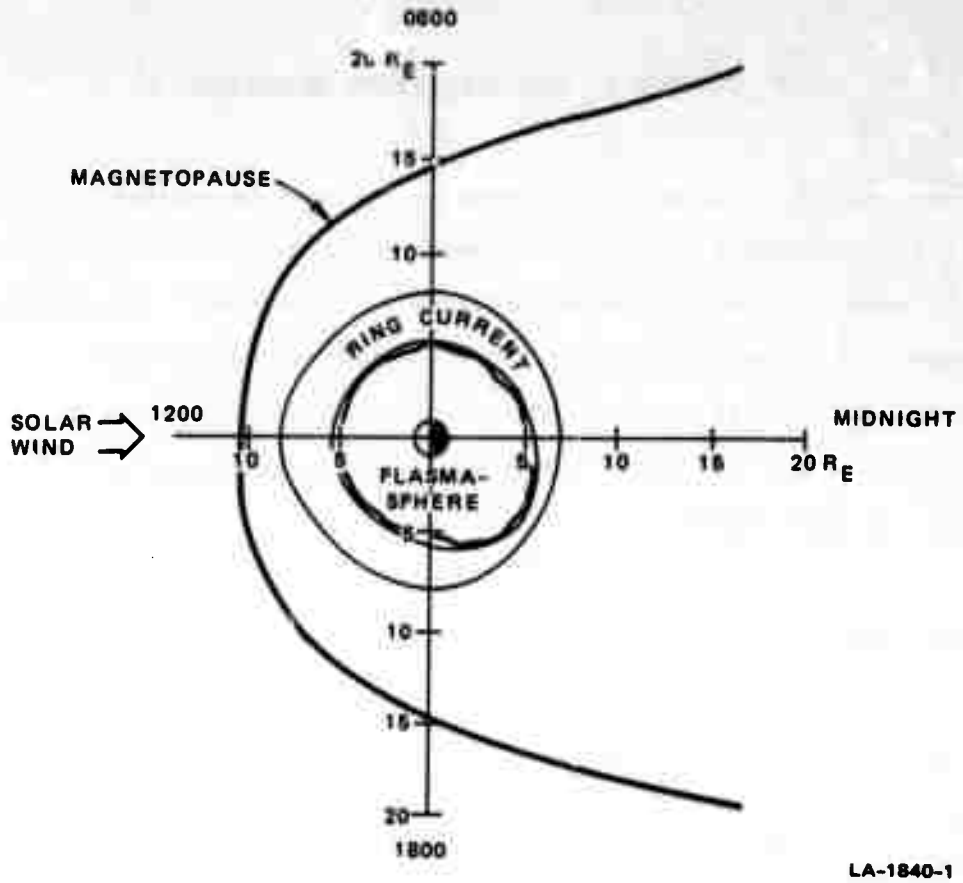

FIGURE 1 OVERALL SCHEMATIC VIEW OF THE MAGNETOSPHERE IN THE GEOMAGNETIC EQUATORIAL PLANE

reflected; and (3) drifting azimuthally around the earth, creating a "ring current," the electrons going east, the protons (80 percent of the ring current) going west.

In addition to the gyrofrequency, the ions and electrons constituting the magnetospheric plasma are subject to electrical restoring forces defined by the natural plasma angular frequencies,

$$\Pi = (Ne^2/m\epsilon_o)^{1/2} \qquad (2)$$

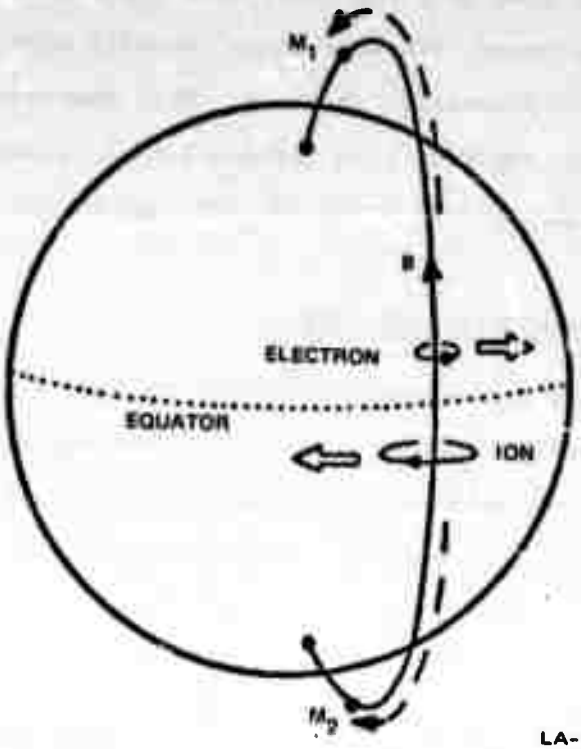

FIGURE 2 THE GYRATION ( ), BOUNCE (---), AND DRIFT ( ) MOTIONS OF A MAGNETOSPHERIC PARTICLE TRAPPED ON A MAGNETIC FIELD LINE

where N is the number density of electrons or ions, and ϵ_o is the permittivity of free space.

In addition to the particles, there are naturally occurring electromagnetic waves propagating in the magnetosphere. VLF waves have right-circular polarization and propagate in the "whistler" mode at a frequency, ω, below the electron cyclotron frequency, Ω_e (i.e., $\omega < \Omega_e$). ULF waves have left-circular polarization and propagate in the "ion-cyclotron" mode below the ion cyclotron frequency, Ω_i (i.e., $\omega < \Omega_i$). The refractive index, n, formulas for these right- and left-circularly polarized waves are as follows:

$$n_R^2 = \Pi_e^2/\omega(\Omega_e - \omega) \qquad n_L^2 = \Pi_i^2/\Omega_i(\Omega_i - \omega) \quad . \qquad (3)$$

These formulas show that as a VLF (ULF) wave approaches the electron (ion) cyclotron frequency, the wave phase velocity approaches zero and the refractive index approaches infinity. This phenomenon is known as cyclotron resonance, since it is a resonance that occurs when the appropriate wave and particle cyclotron frequencies are equal.

B. Cyclotron-Resonance Instability

Consider the wave-particle interaction between a circularly polarized wave of phase velocity, V_p, and a particle spiraling along a magnetic field line with total velocity, V, parallel velocity, $V_{\parallel} = V \cos \alpha$, perpendicular velocity, $V_{\perp} = V \sin \alpha$, and pitch angle, α, as shown in Figure 3.

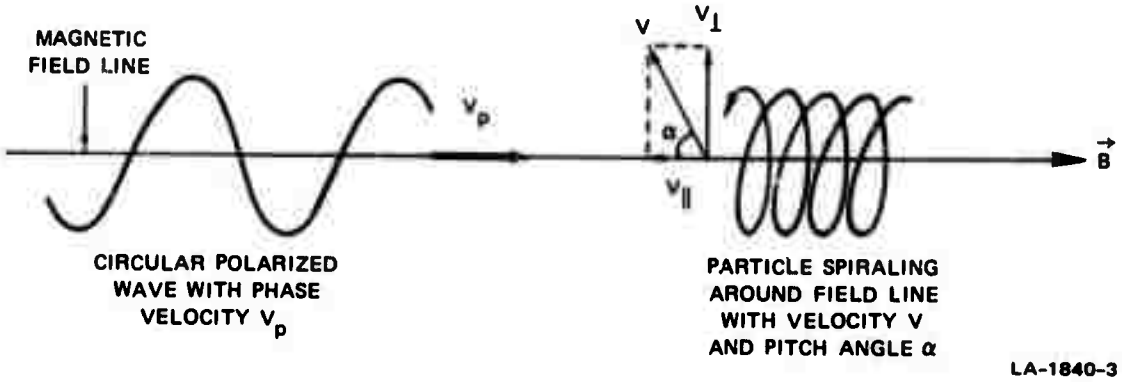

FIGURE 3 SCHEMATIC ILLUSTRATION OF WAVE-PARTICLE INTERACTION CAUSED BY CYCLOTRON RESONANCE

Wave amplification via cyclotron resonance occurs when the motion of the particle Doppler-shifts the wave frequency to the cyclotron frequency of the particle. The resonance parallel velocity of the particle, V_R, is determined by

$$\omega - kV_R = \Omega \qquad (4)$$

where the wave number, $k = 2\pi/\lambda = n\omega/c$. If the particles interacting with waves of appropriate frequency have an anisotropic velocity

distribution, such that $V_\perp$ is greater than $V_\parallel$ on the average, there is a tendency for the wave to grow in amplitude while $V_\perp$ is reduced. This interchange of energy between interacting waves and particles is necessary to maintain conservation of energy and momentum.

In the trapped-particle belts $V_\perp$ is usually greater than $V_\parallel$ since particles with relatively high $V_\parallel$ tend to be lost by collision with particles in the lower atmosphere. A wave interacting with a particle having an excess perpendicular velocity will grow in amplitude while the particle perpendicular velocity decreases and the particle parallel velocity increases, tending to make the particle distribution more isotropic ($V_\perp = V_\parallel$). Thus, on the average, waves will be amplified, and particles, tending to travel more along the field line than before, will no longer be contained and will precipitate from the trapped belt as shown in Figure 4. However, there is a limit to this process, since the wave amplification and particle precipitation depend on the anisotropy of the particle distribution which during amplification becomes more nearly isotropic. Normally, the growth rate of the electromagnetic waves is balanced by convective losses, so that a dynamic equilibrum results between wave amplitude and particle velocity. Convective losses refer to energy carried away from the amplifying region by the amplified wave themselves.

C. Wave Amplification by Cold-Plasma Injection

The growth rate γ of the wave amplitude is[1*]

$$\gamma = 2\pi^2 \frac{\Omega^2}{k}\left(1 - \frac{\omega}{\Omega}\right)^3 F(V_R)\left\{A - \frac{\omega}{\Omega - \omega}\right\} \qquad (5)$$

*References are listed at the end of the report.

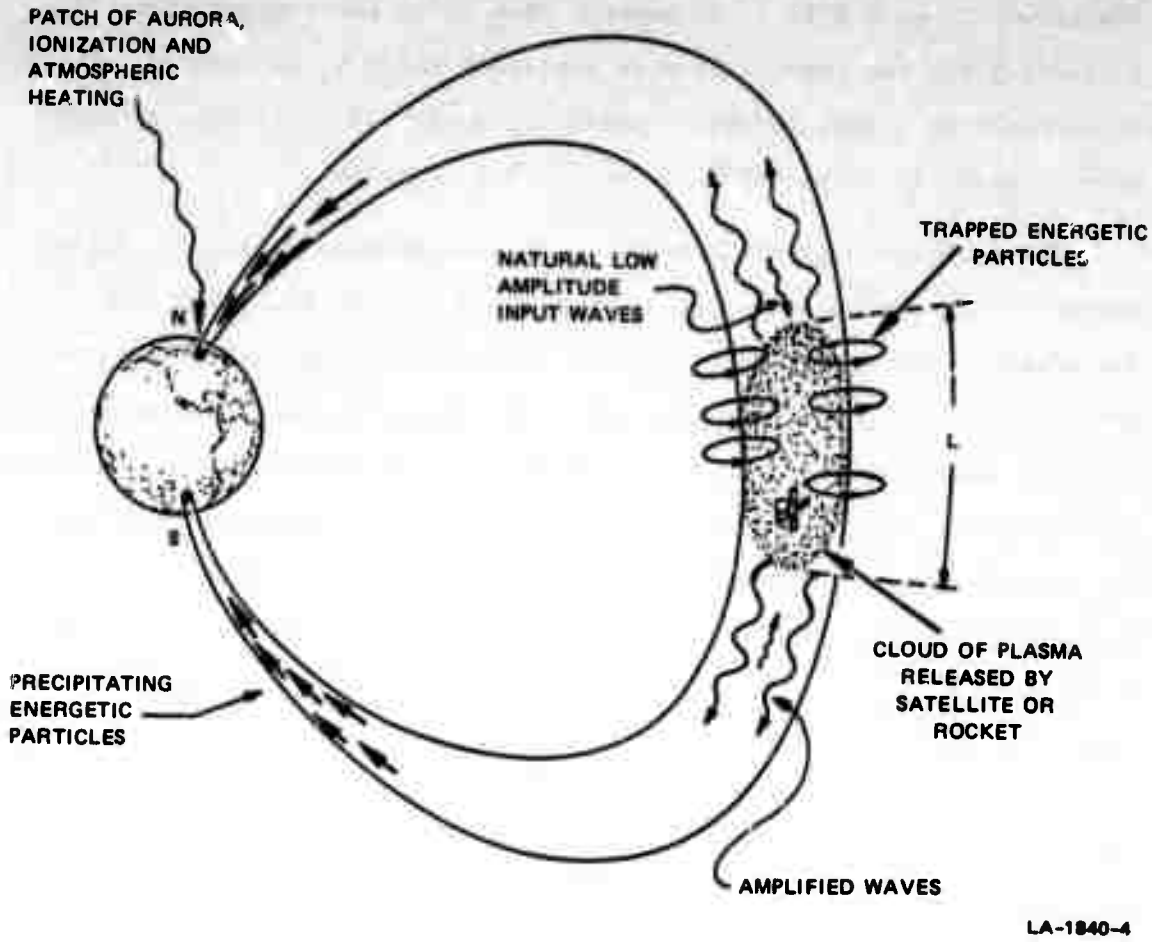

FIGURE 4 SCHEMATIC VIEW OF A SATELLITE PLASMA-INJECTION EXPERIMENT

where the anisotropy of the particle distribution is given by

$$A = \left(\frac{V_\perp^2}{2} - V_\parallel^2 \right) / V_\parallel^2 \qquad (6)$$

and $F(V_R)$ is the number of resonant particles having $V_\parallel = V_R$, where the resonance velocity is given by

$$V_R = V_p \left(\frac{\Omega}{\omega} - 1 \right) \quad . \qquad (7)$$

If $F(V_R)$ can be suddenly increased by decreasing V_R, then significant amplification of naturally occurring electromagnetic waves can be obtained, with accompanying precipitation of particles from the radiation belt. This can be accomplished by the injection of cold (~eV) plasma into the magnetosphere--hot (~keV) plasma is equally effective, but requires excessive injection energy. The injection of cold plasma reduces V_R by increasing the plasma density, N, which increases the plasma frequency, Π, which in turn increases the refractive index [see Eq. (3)] and thus, since $n = c/V_p$, V_p is reduced. This allows the wave to resonate with the more numerous lower-energy particles, increasing $F(V_R)$ and the wave growth rate, γ.

The resulting wave amplitude increase can be accurately calculated if the initial plasma parameters and wave amplitudes are known. Calculation of the concomitant particle precipitation cannot be done as accurately. Hence, definitive experiments could be performed for wave amplification, with close agreement, expected between theory and experiment; and less definitive experiments could be performed for particle precipitation.

Suitable conditions for sizable amplification of naturally occurring ULF and VLF waves occur outside the plasmapause. Here, the cold (~ eV) electrons and ion densitites are of the order of 1 cm^{-3}; the hot (~ keV) plasma consisting mainly of the "ring-current" electrons (~ 20 keV) and protons (~ 20 keV) also has a density of ~1 cm^{-3}. The corresponding cold and hot densities inside the plasmapause are about 10^2 to 10^4 cm^{-3} and about 0.1 cm^{-3}, respectively. A substantial fraction of the energy stored in the magnetosphere (~ 10^{15} joules) is contained in the ring-current particles. For wave amplification one needs to produce a significant increase in the total particle density in a region where there are large fluxes of energetic particles. One also needs an initial total density sufficiently low that a significant density change can be

achieved experimentally. Hence a natural wave amplifying region exists outside the plasmapause (see Figures 1 and 4).

If we consider an amplifying region as shown in Figure 4 having a growth rate γ, a length ℓ, and a wave group velocity V_g, the total wave amplitude gained on one pass through the region is $e^{(\gamma \ell / V_g)}$. Another factor involved in calculating the effect of plasma injection is the coefficient governing the reflection of waves from the plasma-cloud inner surface. If this reflection coefficient is high enough, the system could become an oscillator.

Thus an electromagnetic-wave-amplifying mechanism exists in the magnetosphere outside the plasapause, which can be triggered by the injection of cold plasma and also causes particle precipitation. Since it is necessary to tap only a part of the immense energy of the source region, the amplification process is capable of being an extremely effective one.

V EXPERIMENTAL OBSERVATIONS AND CURRENT THEORY OF ULF AND VLF WAVE-PARTICLE INTERACTION IN THE MAGNETOSPHERE

The amplification of ULF and VLF waves by means of cyclotron resonance was discussed briefly in Section IV above. Observations of such amplification in the natural magnetosphere are discussed below. This section will also comment on more complex aspects of the basic equations that are relevant to magnetospheric amplification of ULF and VLF waves. This problem has received intensive study for some years.[2-5] Recent improvements in the knowledge of both the theory and the relevant properties of the magnetosphere now make it possible to make meaningful detailed calculations concerning the amplification of ULF and VLF waves applicable to real situations. This section will conclude with a discussion of such calculations in connection with lithium plasma injection in the magnetosphere near the geomagnetic equator at L = 6.6.

A. Observations of Natural Wave Amplification in the Magnetosphere

There is ample evidence of wave amplification by wave-particle interaction in the natural magnetosphere. VLF whistlers radiated by lightning discharges propagate from one hemisphere to the other along magnetic field lines. Some whistlers bounce back and forth along the field lines many times, with the reflection loss in the lower ionosphere partially counteracted by wave amplification in the outer magnetospheric portion of the propagation path. Several examples of whistlers showing many "echoes" have been published.[6] An example is given in Figure 5 below.

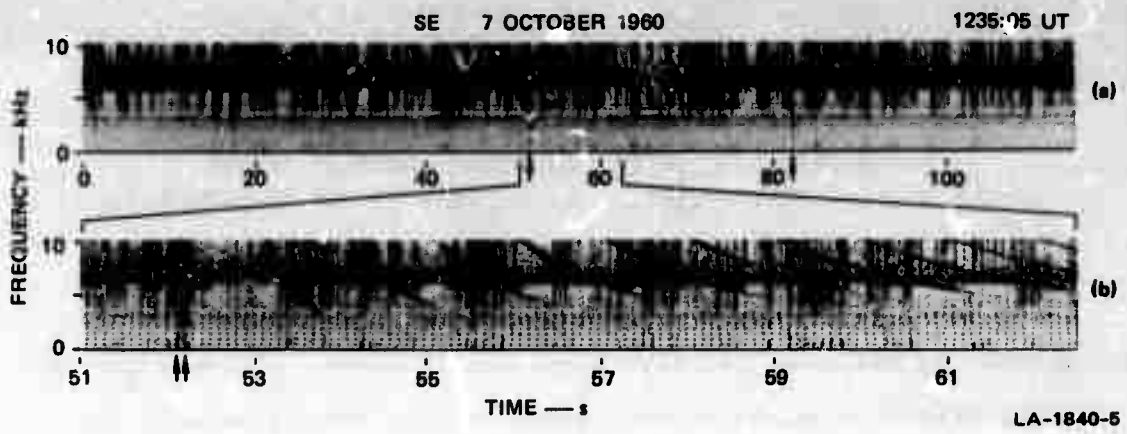

FIGURE 5 LONG-ENDURING WHISTLER ECHO TRAINS. (a) Two even-order echo trains, with whistler source times indicated by arrows superimposed on a background of echoes from a previous whistler with associated periodic emission at a frequency of about 6 kHz. (b) Expanded version of (a) from 51 to 62 s. Whistler is seen to be of the multiflash type, with two main components. From the dispersion of the whistlers measured in (b) and the slope of an echo in the long train of (a) the number of hops in the long train at 50 s is approximately 210. The planetary magnetic index reached 9 during the 24 hours preceding this recording. Source: Ref. 6.

Bands of large-amplitude VLF emissions (with spectral density $\leq 10^{-13}$ W/m^2 Hz) are observed in the frequency range from about 400 Hz to 1.5 kHz in the mid-morning hours at high latitudes. At the most favorable latitudes and local times, Ungstrup and Jackerott[7] find occurrence rates approaching 100 percent. It is generally agreed that these emissions are due to natural amplification of VLF waves by the electron-cyclotron resonance.

Irregular pulsations of diminishing-period (IPDP) phenomena and pearl micropulsation hydromagnetic whistlers are examples of natural ULF wave amplification by the proton-cyclotron resonance. Figure 6 illustrates the pearl micropulsation event in which a ULF wave bounces back and forth along a set of magnetic field lines. As shown in the figure, the pearl micropulsation grows in amplitude, thus clearly indicating the wave-amplification process.

If waves propagating into the magnetosphere are amplified sufficiently, or if previously amplified waves are reflected back into the

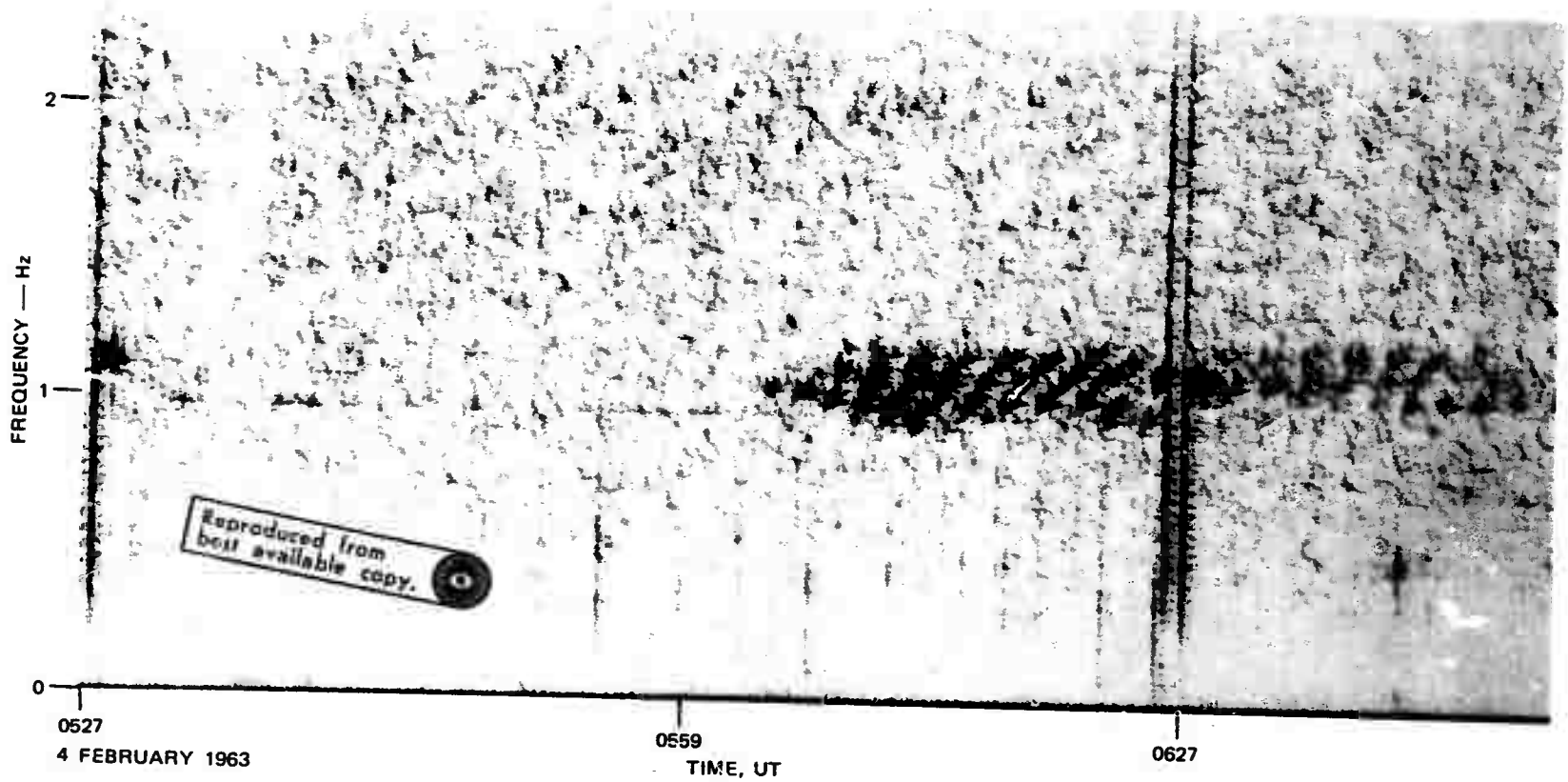

FIGURE 6 SPECTROGRAM OF A PEARL MICROPULSATION EVENT RECORDED AT PALO ALTO, CALIFORNIA, ON FEBRUARY 4, 1963. Source: Ref. 8.

amplifying region, very-large-amplitude waves can result, giving rise to large amounts of energetic particle precipitation. This process is believed to be the principal loss mechanism for energetic protons in the afternoon and early evening hours and for energetic electrons in the late morning hours.

Proton precipitation occurs when azimuthally drifting protons cross the plasmapause near the bulge shown in the evening quadrant in Figure 1, thus entering a region of the plasmasphere of greatly enhanced cold-plasma density, whereas for electrons, there is a gradual increase of cold-plasma density through the morning hours due to injection from the ionosphere below. However, in both cases, precipitation occurs as a result of increased wave amplification associated with increases in cold-plasma density. Estimates of the maximum fluxes of energetic protons and electrons have been made by other investigators,[9,10] to support the contention that increases in the observed natural cold-plasma produce the observed precipitation of protons and electrons. The energy of the precipitated protons heats the ionosphere to produce the stable auroral red arc (SAR arc), while the morning electron energy precipitated averages about 1 erg/cm^2 s.

B. ULF and VLF Theory

1. Consequences of Momentum and Energy Conservation

The physics of wave-particle interaction is outlined in Section IV above. As noted there, wave amplification is produced by cyclotron resonance between waves and energetic particles with anisotropic velocity distributions having excess energy perpendicular to the magnetic field. Since the waves propagate only at frequencies less than the appropriate cyclotron frequency, cyclotron resonance occurs only with energetic particles that have a component of velocity anti-parallel to the wave phase velocity (see Figure 7). In the interaction, conservation

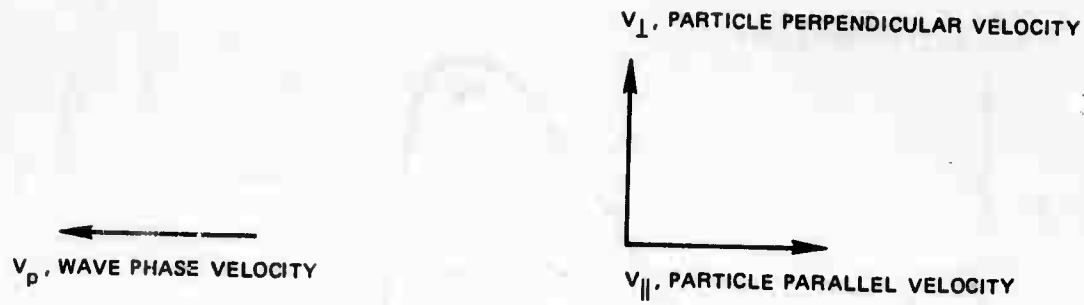

FIGURE 7 VELOCITY RELATIONSHIPS DURING WAVE-PARTICLE INTERACTION VIA CYCLOTRON RESONANCE

of momentum requires an increase in particle parallel velocity. Conservation of energy then requires a decrease in particle perpendicular energy. The conservation equation, together with the resonance condition, Eq. (7), may be combined to relate the changes in wave energy, ΔW_w, particle perpendicular energy, $\Delta W_\perp$, and particle parallel energy, $\Delta W_\parallel$, as follows:

$$\Delta W_w = -\Delta_\perp \left(\frac{\omega}{\Omega}\right) \tag{8}$$

$$\Delta W_\parallel = -\Delta W_\perp \left(\frac{\Omega - \omega}{\Omega}\right) \tag{9}$$

2. Factors Influencing Wave Growth Rate

The wave growth rate, γ, for the cyclotron-resonance instability given by Eq. (5) is shown schematically in Figure 8, which illustrates several features of particular interest.

First, the maximum frequency at which growth can occur is

$$\omega_{max} = \Omega \frac{A}{A + 1} \quad . \tag{10}$$

In most cases the frequency of maximum wave growth is slightly less than ω_{max}. For wave growth to occur, we must have $A > \omega/(\Omega - \omega)$. That is, there is a minimum anisotropy for wave growth.

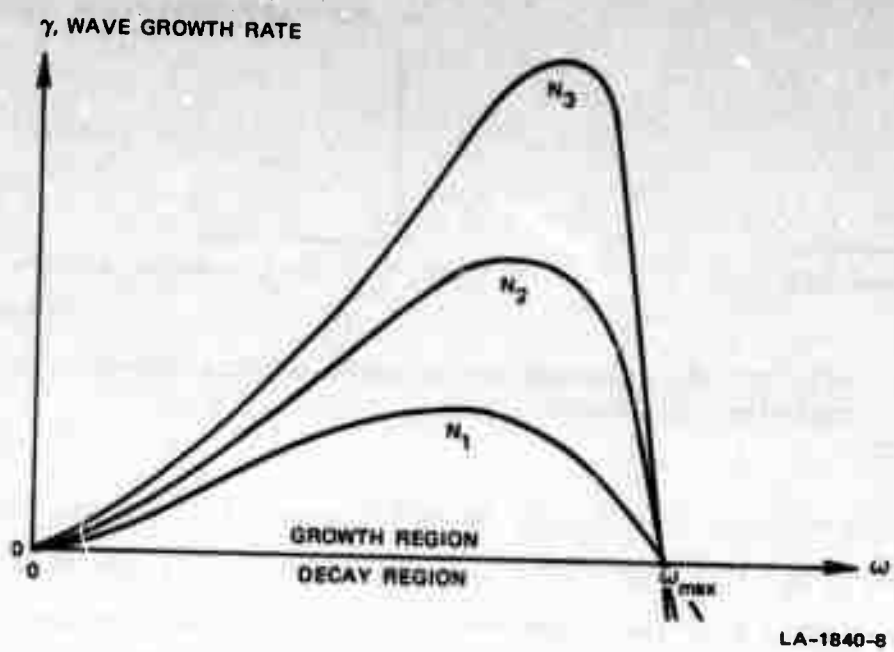

FIGURE 8 WAVE GROWTH RATE vs. FREQUENCY

To illustrate the variation of γ with the density of injected plasma we must consider the form of F(V)--i.e., the number of particles available for resonance when $V = V_R$--as shown schematically in Figure 9 and in the proton data in Section V-B-4 (Figure 10). Let N_1 be the natural ambient plasma density. N implies a plasma frequency Π, and refractive index n, which lead to a phase velocity V_1, and via Eq. (7) to a resonance velocity $V_R = V_1$. The wave growth rate is then determined by $F(V_1) = F_1$. As mentioned in Section IV, the growth rate is balanced by convective losses under normal conditions. If the plasma density in the amplifying region is increased by plasma injection from N_1 to N_2 or N_3, then the corresponding increases in F(V) from F_1 to F_2 or F_3 cause large increases in γ and hence in wave amplitude and particle precipitation.

If we let $\omega \rightarrow 0$, then $V_R \rightarrow \infty$ and $F(V_R) \rightarrow 0$, which makes $\gamma \rightarrow 0$ as shown in Figure 8.

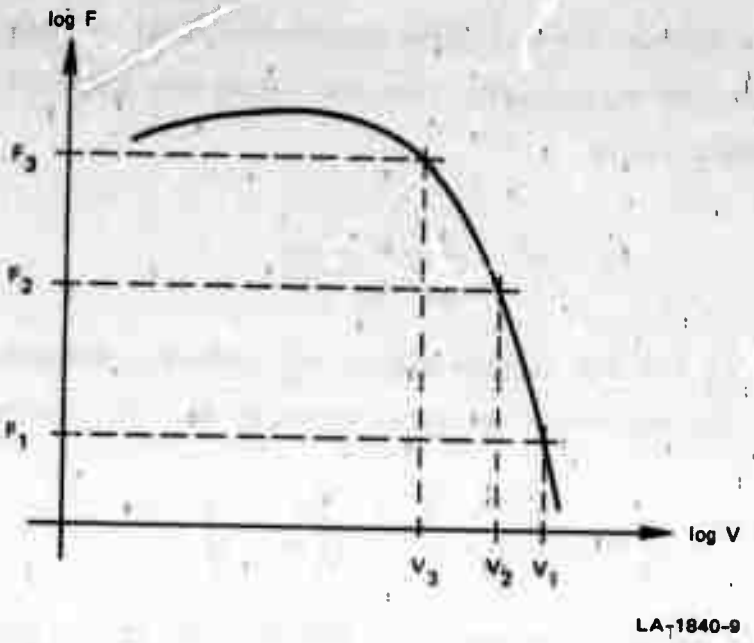

FIGURE 9 SCHEMATIC REPRESENTATION OF THE NUMBER OF PARTICLES AVAILABLE FOR RESONANCE, F(V), vs. THE PARTICLE VELOCITY, V

3. Cold-Plasma Density Required for Amplification

It is important to calculate the total amount of wave growth that would be expected if realistic amounts of cold plasma were injected into previously measured energetic-particle distributions. This requires a knowledge of the energetic-particle flux and anisotropy versus energy. While the detailed information on the anisotropy is not readily available, a reasonable estimate may be made and used together with measured fluxes, such as that shown in Section V-B-4 (Figure 10). From this information, the amount of cold plasma required to make a major perturbation in the energetic particles can be readily computed. Such calculations are being carried out by Cornwall, by Liemohn, and by Brice and Lucas.

A rough estimate of the amount of cold plasma required may be obtained as follows: If lithium ions are injected in sufficient numbers

to dominate the average ion mass (see discussion later in this subsection regarding the choice of lithium), then the refractive index of a ULF wave is given approximately by

$$n^2 = \frac{\Pi^2_{Li}}{\Omega_{Li}(\Omega_{Li} - \omega)} \quad . \tag{11}$$

where Π_{Li} and Ω_{Li} are the lithium plasma and cyclotron frequencies respectively. The resonance velocity, given by Eq. (7), becomes

$$V_R = -V_p\left(\frac{\Omega_p}{\omega} - 1\right) = -\frac{c}{n}\left(\frac{\Omega_p}{\omega} - 1\right) \tag{12}$$

where Ω_p is the proton gyrofrequency. For example, if $\omega = 0.8\ \Omega_{Li} = 8/70\ \Omega_p$, then the proton resonance velocity square from Eq. (12) can be used to calculate the parallel resonance proton energy, E_R:

$$E_R = \frac{1}{2} m_p V_R^2 \approx \frac{1.7}{N_{Li}} \frac{B^2}{2\mu_o} \tag{13}$$

where $m_{Li} \approx 7 m_p$, m_{Li}, and m_p being the lithium and proton mass, respectively. Equating this resonance energy with the mean energetic proton energy, $\bar{E}_p$, we can obtain an estimate of the desired lithium density:

$$N_{Li} \approx \frac{(1.7)\ B^2}{2\mu_o \bar{E}_p} \tag{14}$$

For an equatorial distance of 6.6 earth radii corresponding to a synchronous satellite orbit, this reduces to

$$N_{Li} \approx \frac{46}{\bar{E}_p} \text{ ions cm}^{-3} \tag{15}$$

where $\bar{E}_p$ is given in keV.

For wave-particle interaction with electrons, the mass of the ion is irrelevant; and the total electron density, N_e, required to make the parallel resonance energy equal to the characteristic energetic electron energy, $\bar{E}_e$, is, from an argument similar to that above,

$$N_e = \frac{B^2}{2 \mu_o A (A + 1)^2 \bar{E}_e} \tag{16}$$

where the wave frequency is set equal to the maximum frequency at which growth occurs ($\omega = \omega_{max}$). For an anisotropy of 0.5 at the synchronous orbit, we have

$$N_e \approx \frac{25}{\bar{E}_e} \text{ el cm}^{-3} \tag{17}$$

where $\bar{E}_e$ is given in keV. For an anisotropy of 0.1, we have

$$N_e \simeq \frac{240}{\bar{E}_e} \text{ el cm}^{-3} \quad . \tag{18}$$

These densities of lithium ions or electrons need to extend over an area perpendicular to the magnetic field sufficient to make a "duct" to guide the ULF or VLF waves respectively, and long enough along the field line for substantial total wave growth. The minimum required cross-sectional area (perpendicular to the field line) should have a diameter of the order of a wavelength in the enhanced-density region, which is thus much smaller for the higher-frequency VLF waves than for ULF waves. At synchronous orbit with $\omega \simeq 0.8\ \Omega_{Li}$ and $N_{Li} \approx 3\ \text{cm}^{-3}$, the ULF wave-length is 1220 km, while for $\omega = 0.3\ \Omega_e$, the VLF wavelength is 8.8 km.

If the "required" electron and lithium ion densities were injected, and the energetic electrons and protons had the same density and mean energy, then the logarithmic VLF wave growth would be larger than that for ULF waves by about the square root of the proton-electron mass

ratio, or roughly 43. Thus a ULF wave gain of 30 dB would correspond to a VLF wave gain of 1300 dB. Thus, for the same growth, a somewhat smaller number of electrons could be injected. If the energetic-particle distribution were relatively soft--i.e., $F(V_R) \propto V_R^{-6}$--then the same wave growth should occur at ULF and VLF if the electron density were smaller than the lithium ion density by a factor of $(43)^{2/6}$ or 3.5. For a harder spectrum with $F(V_R) \propto V_R^{-4}$, the electron density could be smaller by a factor of $(43)^{2/4}$, or 6.5. If $F(V_R)$ varies as V_R^{-x}, then the wave gain (in dB) will vary as $N^{x/2}$ where N is the injected-plasma density.

Additional factors that also need to be considered are the wave attenuation during propagation through the lower ionosphere, which is expected to be quite small (probably negligible) at ULF but may be 30 or 40 dB at VLF.

4. ULF Wave Amplification by Injection of Cold Lithium Plasma at L = 6.6 Near the Geomagnetic Equatorial Plane

The basic mechanism for the interaction of energetic protons with ULF waves has been described above: injection of cold plasma lowers the ULF wave speed to the point where the bulk of the energetic protons can be in cyclotron resonance with the waves. The great virtue of lithium is that at ULF frequencies the ion mass is the important factor in slowing down the wave. Hence, each lithium ion is about seven times more effective than a proton since it is about seven times more massive. However, the cold-plasma ion must be light enough to be readily moved by the ULF waves, or else the resonance interaction will be destroyed. For this reason barium ions, being about 20 times more massive than lithium ions, are not useful in ULF amplification; however barium can be quite useful for VLF amplification. Using hydrogen is impractical because of the high energy required for ionization, but lithium meets nearly all the requirements. Lithium is readily ionized by sunlight, and will make

a sufficiently large plasma cloud (hundreds or even thousands of kilometers across). Furthermore, the technology of lithium atom release with thermite canisters is well developed.

Consider a technologically feasible lithium-release experiment in which a lithium ion cloud of density $N_{Li} \approx 3\ km^{-3}$ fills a field-aligned tube some 400 km in diameter and about 7,000 km long as illustrated schematically in Figure 4. To calculate the growth (gain) experienced by a ULF wave on a single pass along the lithium-ion column we simply calculate the growth rate at a sufficiently large number of points along the wave path (which coincides with the column of lithium ions) and sum up the individual contributions. If γ is sufficiently uniform over the amplifying region, then the wave-amplitude growth $\approx e^{(\gamma \ell / V_g)}$, or total gain $\approx 8.7\ (\gamma \ell / V_g)$ dB, where ℓ is the length of the amplifying region and the wave group velocity,

$$V_g = \partial (kV_p)/\partial k \quad . \tag{19}$$

Calculations of wave amplification are critically dependent on the number of particles available for resonance $F(V_R)$ in Eq. (5). Over the past several years, observations from several spacecraft have made it possible to assemble an accurate average measurement of $F(V_R)$ applicable to the ULF wave-proton interaction case considered here. The compilation of data[11] shown in Figure 10 was used to make the present calculations. It is also important to note that a study of 6 months of data showed that while proton fluxes are occasionally higher than those shown in Figure 10, they are seldom lower.

Wave-growth calculations were made by Cornwall using the data of Figure 10 and an anisotropy $A = 1/2$, which is reasonable in view of current observational data supplied by Frank.[11] The result was a linear growth rate of 6.6×10^{-3} dB/km. Over the 7,000-km path length this

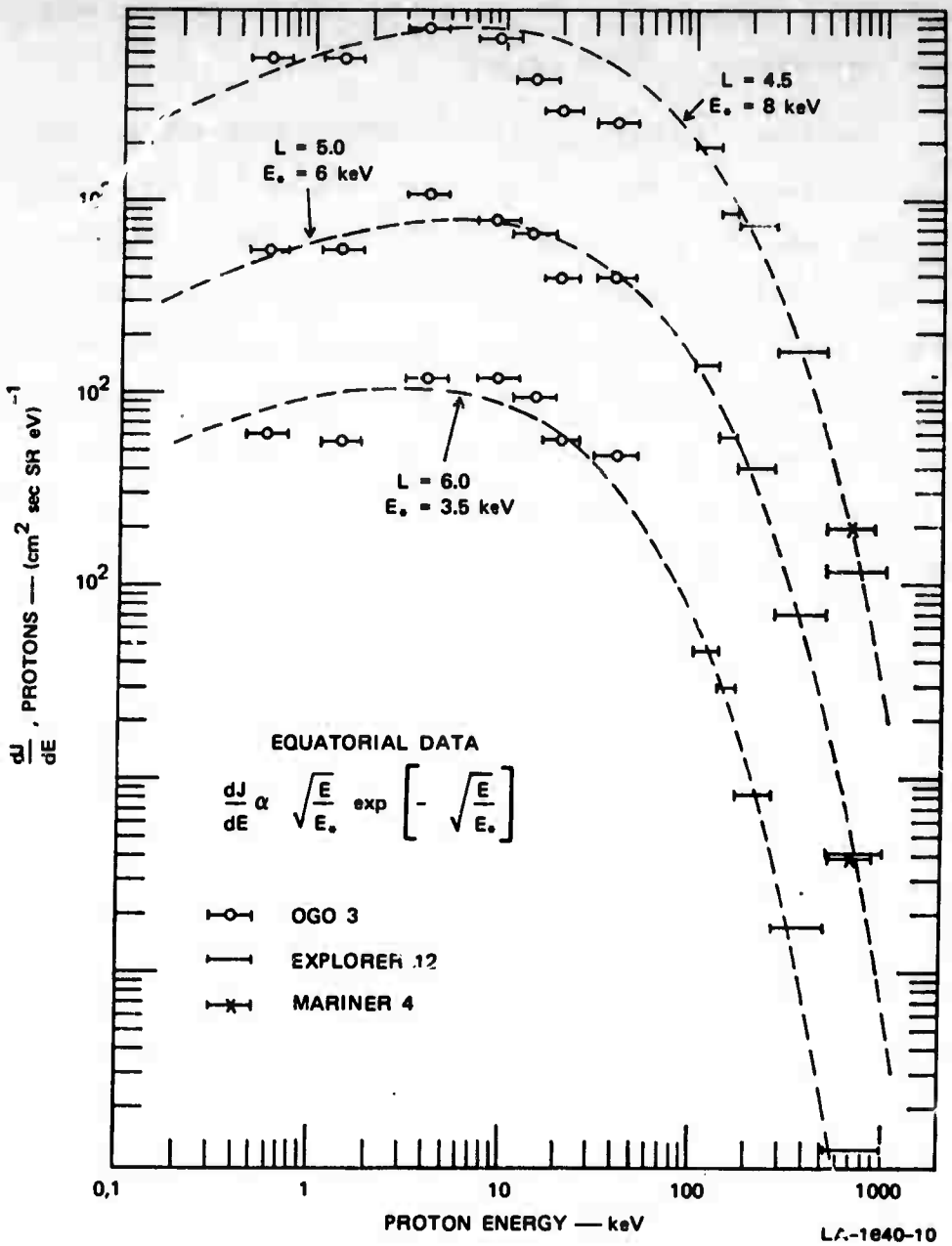

FIGURE 10 DIRECTIONAL, DIFFERENTIAL SPECTRUMS OF PROTON INTENSITIES OVER THE ENERGY RANGE 200 eV TO 1 M V, AND MIRRORING AT THE MAGNETIC EQUATOR, AS COMPILED FROM OBSERVATIONS WITH OGO 3 (Ref. 12), EXPLORER 12 (Ref. 13). The ordinate scales for the proton spectrum at L = 4.5, 5.0, and 6.0 have been displaced by a factor of 10, as noted on the left ordinate scale — i.e., maximum differential intensities are $\sim 10^3$ protons $(cm^2\ sr\ eV)^{-1}$ at ~10 keV for each spectrum. The horizontal bars for each measurement indicate the effective energy bandpasses of the instruments. Approximate values for E_o are 8.0, 6.0, and 3.5 keV at L = 4.5, 5.0, and 6.0, respectively. Source: Ref. 11.

amounts to about a 45-dB wave gain. This 45-dB figure refers to a frequency of $\omega = 0.8\ \Omega_{Li} \approx 0.2$ Hz, where the wave gain is maximized for the given conditions. This frequency is also about the maximum frequency for amplification by cold-plasma injection at L = 6.6. While there are uncertainties in the calculation--e.g., a 30 percent uncertainty in the satellite measurement of $F(V_R)$--a 30 to 40 dB gain is reasonable. Considering the region outside the plasmapause from L = 4 to L = 7 and within 30 degrees of the geomagnetic equatorial plane, useful amplification could be obtained in the 0.1-to-5-Hz frequency range.

While this calculation by Cornwall is used as an illustration here, it should be noted that several researchers, including Brice (Cornell University) Cornwall (UCLA and Aerospace), and Liemohn (Battelle-Northwest) have computer programs for making similar detailed wave-amplification calculations. However, more theoretical work needs to be done to extend and confirm the type of calculation made above, and more spacecraft data should be reduced to forms useful or inputs in making theoretical calculations.

VI DESIGN OF EXPERIMENTS TO INVESTIGATE WAVE-PARTICLE INTERACTION PHENOMENA

Experiments are now feasible to investigate ULF and VLF wave amplification, and particle precipitation caused by artificial cold-plasma injection. The experimental concepts described below are sound and there appears to be no fundamental uncertainty or obstacle. There are, however, analyses of existing satellite data and instrumentation capabilities that are essential in order to define and design these experiments in detail.

Successful cold-plasma injection experiments must meet several general conditions. The volume into which the plasma is injected must be outside the plasmapause and near the geomagnetic equatorial plane. The ambient thermal plasma density prior to injection must be low enough that the injected plasma will be a major perturbation. The ambient energetic particle flux must not be too low or too disturbed. Drift separation between the injected plasma cloud and the spacecraft measuring the cloud parameters is undesirable.

A. ULF Wave Amplification

As has been shown in Section V-B, the injection of lithium ions into the energetic proton environment at synchronous altitude can produce wave particle interaction. This interaction will remove some of the energy from the ambient protons for amplification of ULF waves in the 0.1-to-5 Hz range. This modifies the proton angular distribution so that some of the protons will precipitate.

The experiments required to measure the amount of ULF wave amplification and proton precipitation are listed in Table 2. Each experiment is discussed below.

Table 2

MEASUREMENTS FOR ULF WAVE AMPLIFICATION EXPERIMENTS

Measurement	Observation Platform
Proton environment in amplifying volume	Spacecraft
Li injection	Spacecraft
Li ions	Spacecraft Ground
Li neutrals	Ground
ULF waves	Spacecraft Ground
Proton precipitation	Ground

1. Proton Environment

To accurately compare theory with experimental results, it is necessary to know the phase-space distribution of the ambient protons in the volume where the ULF wave amplification is to take place. Thus, the pitch-angle distribution, energy distribution, and flux of protons must be measured. The type of instrument required for these measurements has been flown on a number of spacecraft.

The ULF wave amplification experiment should not be performed during highly disturbed times or when the energetic proton flux is unusually low. However, this does not require a real-time capability for monitoring the proton environment in order to select a time for lithium

injection. Extensive synchronous-orbit proton data have been taken. These data must be examined to determine indicators, such as K_p, so that we can determine when the probability of having an acceptable proton environment is very high.

2. Lithium Injection

A volume of ionized lithium is needed at the equator at synchronous orbit. The concentration must be $\gtrsim 3$ cm^{-3} over a region hundreds of km in radius perpendicular to the magnetic field lines. Injection by thermite canister at the equator is certainly practical. Injection from a rocket-borne shaped charge from just above the atmosphere may also be practical. Efficiencies and payload weights for lithium injection must be checked in more detail.

The cold-plasma background must be low enough that the injected lithium is a major perturbation. A study of existing data is needed in order to select magnetic conditions and times of high probability of an acceptably low-density cold-plasma background.

3. Lithium Ions

To make a meaningful comparison of theory and experimental results, the concentration and distribution of injected lithium ions in the equatorial region are needed. The convection and striation of the ion cloud may be important.

The release time needs to be selected to minimize convection effects. Convection relative to corotation with the earth will probably be favorable from midnight through dawn to noon. Available plasma-convection and electric-field data need to be studied in order to select times and magnetic conditions favorable for lithium injection.

Lithium ions can be measured in the release cloud with an in situ plasma detector. This will probably not measure striations, and the lithium ions may convect away from the spacecraft with the plasma detector. Hence, an in situ satellite plasma detector will probably not adequately measure the distribution of lithium ions.

Solar X-ray fluorescence of lithium ions will produce weak far-UV and visible radiation. A calculation needs to be made to see if this is a feasible technique for obtaining a two-dimensional plot of the lithium-ion distribution. The UV observations would have to be made with a photometer on a spacecraft, while the visible observations could be made from the ground.

4. Lithium Neutrals

The lithium inventory must be measured in order to determine the amount of lithium injected. This can be performed from ground-based photometers. The loss of lithium as a function of space and time gives information on the production and initial location of lithium ions. Consequently, an analysis of the sensitivity of lithium photometry should be made.

5. ULF Waves

ULF waves of 0.1 to 5 Hz can be measured on the ground at the ends of the field lines that pass through the amplifying volume. Magnetometer sensitivities of about 10^{-3} gamma are practical. In order to measure the ambient ULF noise and to obtain an amplification factor, the ULF waves also need to be measured on a spacecraft near the plasma cloud. Because of spacecraft instrument noise, a spacecraft magnetometer is limited to a sensitivity of about 10^{-1} gamma.

6. Proton Precipitation

The number of protons placed on the loss cone by the wave-particle interaction is very difficult to measure at the equator where the loss cone has an apex angle of only a few degrees. The pitch-angle distribution needed for the proton environment measurement (Section VI-A-1, above) can have a resolution of tens of degrees.

The precipitated protons will excite and ionize the E region at the ends of the field lines. Techniques such as backscatter radar, phase sounder or Hβ photometry (at night) may be useful. An analysis of the excitation and ionization by the predicted precipitating protons is needed to determine whether they can be observed over the ambient environment.

B. VLF Wave Amplification

Injection of cold plasma in the equatorial region at synchronous orbit should result in the amplification of VLF waves by the ambient energetic electrons. The amplification may occur somewhere between 100 Hz and 15 kHz, but most likely between 400 and 1.5 kHz. The wave amplification removes energy from the ambient electrons, resulting in a modification of the electron angular distribution, causing some of the electrons to precipitate.

The experiments required to measure the amplification of VLF waves and the electron precipitation are listed in Table 3. Each experiment is discussed below.

Table 3

MEASUREMENTS FOR VLF WAVE-AMPLIFICATION EXPERIMENT

Measurement	Observation Platform
Electron environment in amplifying volume	Spacecraft
Cold-plasma injection techniques	Spacecraft
Ion distribution	Spacecraft Ground
Neutral distribution	Ground
VLF waves	Spacecraft Ground
Electron precipitation	Ground Balloon

1. Electron Environment

To make meaningful comparisons of theory and experimental results, it is necessary to know the phase-space distribution of ambient electrons at the equator in the volume in which the VLF wave amplification is to take place. Thus, the angular distribution, energy distribution, and flux of electrons must be measured. The type of instrument required has been flown on a number of spacecraft.

The VLF wave-amplification experiment should not be performed during highly disturbed times or when the electron flux is unusually low. A real-time capability for monitoring the electron environment to select a time for ion injection is not required. Much synchronous-orbit electron data have been taken. It must be examined to determine indicators, such as K_p, so that we can determine when the probability of having an acceptable electron environment is very high.

2. Cold-Plasma Injection Techniques

For VLF amplification a volume of cold plasma is needed at the equator at synchronous orbit, the electrons being the important component. A concentration of about ≥ 10 el cm^{-3} is needed over a region tens of kilometers in radius perpendicular to the magnetic field lines. The free electrons can be obtained from the injection of lithium or barium ions, for example. Injection of lithium or barium from a canister at the equator is practical. It appears possible that rocket-borne shaped charges fired from above the atmosphere can achieve the necessary concentration, under appropriate magnetospheric conditions.[14] Large-size satellite barium release payloads can be readily made. Efficiencies and payload weights for lithium injection must be checked in more detail.

The cold-plasma background must be low enough so that the injected cold electrons are a major perturbation. A study of existing data is needed in order to select magnetic conditions and times when the probability of an acceptably low cold-plasma background is very high.

3. Ion Distribution

In order to compare calculated and observed wave-amplitude growth, it is necessary to know the concentration and distribution of ions injected into the equatorial region. Consequently, convection and striating of the ion cloud may be important.

Release time needs to be selected to minimize convection effects. Convection relative to corotation with the earth will probably be favorable from midnight through dawn to noon. Available plasma convection and electric-field data need to be studied in order to select times and magnetic conditions favorable for injection.

Barium ions can easily be measured by ground-based optical techniques. The problems of measuring the distribution of lithium ions are discussed above for ULF wave amplification.

4. Barium or Lithium Neutrals

The barium or lithium inventory must be measured in order to determine the amount injected. This can be performed from ground-based photometers. The loss of lithium or barium as a function of space and time gives information on the production and initial location of lithium or barium ions. Consequently, an analysis of the sensitivity of lithium or barium photometry should be made.

5. VLF Waves

VLF waves of ~400 Hz to 1.5 kHz need to be measured on a spacecraft to determine the amplification factor. Ground-based VLF receivers can be used at the ends of the field lines to measure VLF amplification; however, the attenuation in transit through the ionosphere makes the ground-based data difficult to interpret.

6. Electron Precipitation

The amount of electrons placed in the loss cone by the VLF wave amplification is very difficult to measure at the equator where the loss cone has an apex angle of only a few degrees. The angular distribution needed for the electron-environment measurement can have a resolution of tens of degrees.

The precipitated electrons will excite and ionize the D and E regions of the ionosphere at the ends of the field lines. Techniques such as backscatter radar, phase sounder, or N_2^+ 1N photometry (at night) may work. N_2^+ 1N photometry refers to the observation of the "first

negative" optical and near-ultraviolet emission bands of the N_2^+ nitrogen molecular ion. The bands occur in the range of 2987 to 5864 Å.

C. Wave-Transmission Studies

On occasion, a wave-particle interaction at VLF frequencies is sufficiently strong to be self-sustaining, once the emission process is stimulated or triggered by an input wave. These "discrete emissions" often show an apparent saturation in amplitude and last typically about 1 s, with extreme examples lasting about 20 s. Discrete emissions are known to be associated with the dumping of substantial quantities of electrons into the upper atmosphere, as detected by measurements of bremsstrahlung X-rays in balloons.

The purpose of ground-based wave-transmission studies is to determine the optimum input signal frequency and waveform for stimulating emissions and electron precipitation, to determine how frequently this process occurs, and whether the emission of waves significantly alters the properties of the energetic particles. For example, we must determine if one emission substantially reduces the wave growth rate, inhibiting subsequent emission, and if so, what the "recovery time" is. The wave-transmission experiments also permit general studies of nonlinear wave phenomena in the magnetosphere. We might ask if it is possible to simultaneously stimulate emissions at two different frequencies, and if so, whether the nonlinear effects include significant wave-wave coupling and production of low-frequency waves at the difference frequency.

Two ground-based wave-transmission facilities are presently being constructed: one at Siple, Antarctica with conjugate receiving facilities at Roberval, Canada under NSF sponsorship, and the other at Port Heiden, Alaska with conjugate receiving facilities at Dunedin, New Zealand under Navy sponsorship.

A sub-LF satellite-borne wave transmission experiment has been proposed by the Navy for studying the generation and propagation of sub-LF waves in the ionosphere in order to determine the feasibility of direct satellite communications with submerged submarines.

REFERENCES

1. C. F. Kennel and H. E. Petschek, "Limit on Stably Trapped Particle Fluxes," J. Geophys. Res., Vol. 71, No. 1, p. 1 (1966).

2. N. Brice, "Artificial Enhancement of Energetic Particle Precipitation Through Cold Plasma Injection: A Technique for Seeding Substorms?" J. Geophys. Res., Vol. 75, No. 25, p. 4890 (1970).

3. J. M. Cornwall, "Precipitation of Auroral and Ring-Current Particles by Artificial Plasma Injection," Rev. Geophys. and Space Phys. (in press, 1972).

4. H. B. Liemohn, "Cyclotron-Resonance Amplification of VLF and ULF Whistlers," J. Geophys. Res., Vol. 72, No. 1, p. 39 (1967).

5. A. Hasegawa, "Plasma Instabilities in the Magnetosphere," Rev. Geophys. and Space Phys., Vol. 9, No. 3, p. 703 (1971).

6. R. A. Helliwell, Whistlers and Related Ionospheric Phenomena (Stanford Press, Stanford, California, 1965).

7. E. Ungstrup and I. M. Jackerott, "Observations of Chorus below 1500 Hz at Godhavn, Greenland, from July 1957 to December 1961," J. Geophys. Res., Vol. 68, No. 8, p. 2141 (1963).

8. A. C. Frazer-Smith and K. R. Roxburgh, "Triggering of Hydromagnetic Whistlers by Spherics," Planet. Space Sci., Vol. 17, p. 1310 (1969).

9. J. M. Cornwall, F. V. Coroniti, and R. M. Thorne, "Turbulent Loss of Ring Current Protons," J. Geophys. Res., Vol. 75, No. 25, p. 4699 (1970).

10. N. Brice and C. Lucas, "Influence of Magnetospheric Convection and Polar Wind on Loss of Electrons from the Outer Radiation Belt," J. Geophys. Res., Vol. 76, p. 900 (1971).

11. G. Pizzella and L. A. Frank, "Energy Spectrum for Proton (200 eV $\sim E \lesssim 1$ MeV) Intensities in the Outer Radiation Zone," J. Geophys. Res., Vol. 75, p. 1269 (1970).

12. L. A. Frank and H. D. Owens, "Omnidirectional Intensity Contours of Low-Energy Protons ($0.5 \lesssim E \lesssim 50$ keV) in the Earth's Outer Radiation Zone at the Magnetic Equator," J. Geophys. Res., Vol. 75, p. 1269 (1970).

13. L. R. Davis and J. M. Williamson, "Outer Zone Protons," in Radiation Trapped in the Earth's Magnetic Field, Billy McCormac, ed. (Reidel, Dordrecht, Holland, 1966).

14. G. B. Carpenter, "Optical, Magnetic and Radio Measurements in Support of the Oosik Experiment," Final Report, Contract N00014-72-C-0394, ARPA Order No. 2141, SRI Project 1840, Stanford Research Institute, Menlo Park, Calif. (August 1972).